The effect of T6 heat treatment on the tensile, impact, and fatigue properties of Al6061-fly ash composites

Zainun Achmad[1*], Al Emran bin Ismail[2], Harjo Seputro[1] and Eka Marliana[1]

[1] Department of Mechanical Engineering, Faculty of Engineering, Universitas 17 Agustus 1945 Surabaya, **Indonesia**
[2] Faculty of Mechanical and Manufacturing Engineering, Universiti Tun Hussein Onn Malaysia, **Malaysia**

*Corresponding Author: zainun@untag-sby.ac.id
Received: 02 December 2025; *Revised:* 24 March 2026; *Accepted:* 15 April 2026

Cite this https://doi.org/10.24036/teknomekanik.v9i2.50672

Abstract: This study investigates the effect of controlled precipitation hardening on the mechanical behavior of Al6061–fly ash metal matrix composites fabricated using stir casting and subjected to T6 heat treatment. The specimens underwent solution treatment at 510°C for 1 and 2 hours, followed by oil quenching and artificial aging at 120°C, 140°C, and 160°C for 2 hours. Tensile, Rockwell hardness, impact, and fatigue tests were used to assess the mechanical characteristics, in accordance with ASTM standards, and were supported by microstructural and SEM studies. The findings indicate that T6 treatment greatly improves strength and fatigue tolerance compared with the untreated state. The highest tensile strength and impact energy were achieved under the T6-A2 condition (510 °C for 2 h + aging at 120 °C for 2 h), whereas the longest fatigue life was obtained under the T6-B1 condition (510 °C for 1 h + aging at 140 °C for 2 h). This shows a good balance between strength and toughness, which is related to the formation of fine Mg_2Si precipitates and enhanced interfacial bonding. Aging at 120°C resulted in the highest hardness at 510°C (2 hours). Over-aging reduced ductility and impact resistance because of precipitate coarsening. For durable aluminum–fly ash composites, these results show a distinct link between processing, microstructure, and material characteristics.

Keywords: Al6061; fly ash; T6 heat treatment; tensile strength; impact energy; fatigue strength

1. Introduction

The demand for engineering materials offering high performance, economic feasibility, and environmental sustainability has increased significantly across various industrial sectors [1], [2]. In response to these challenges, researchers continue to develop advanced materials that not only exhibit superior mechanical properties but also promote resource efficiency and waste utilization. Among these materials, metal matrix composites (MMCs) have gained considerable technological and commercial importance due to their ability to combine lightweight characteristics with enhanced mechanical performance [3], [4], [5], [6].

Aluminum alloys and aluminum-based Metal Matrix Composites (MMCs) are widely used in engineering applications due to their low density, high specific strength, good corrosion resistance, and excellent formability. These materials are widely used in aerospace and aircraft structures, automotive components, military equipment, electronic housings, and biomedical devices, where weight reduction and mechanical reliability are critical. The addition of ceramic reinforcements further expands their potential application in tribological and load-bearing components such as brake rotors, pistons, cylinder liners, and wear-resistant parts [1], [3].

Various ceramic reinforcements, including SiC, Al_2O_3, B_4C, TiC, graphite, and fly ash have been introduced into aluminium matrices to enhance mechanical and tribological properties. While reinforcements such as SiC and Al_2O_3 significantly improve hardness and wear resistance, they may reduce ductility and increase production cost. In contrast, fly ash, an industrial waste by-product of coal combustion, offers advantages in terms of low density, cost-effectiveness, and environmental sustainability [6], [7], [8], [9]. However, challenges remain regarding uniform particle distribution and interfacial bonding between fly ash particles and the aluminium matrix, which directly affect load transfer efficiency and fatigue performance [10], [11], [12].

Among various fabrication techniques, stir casting is considered one of the most economical and scalable methods for producing aluminium matrix composites, particularly for structural applications [4], [13]. Nevertheless, achieving homogeneous reinforcement dispersion and strong matrix–particle interfacial bonding requires careful control of process parameters, alloy chemistry, and surface modification techniques. Previous studies have shown that magnesium addition and electroless coating treatments can improve wettability and enhance interfacial adhesion between fly ash particles and molten aluminium [14].

Despite the extensive research that has been conducted on aluminium matrix composites and precipitation-hardened Al–Mg–Si alloys [1], [2], [3], [4], [5], [15], [16], only a small number of studies have methodically combined the electroless surface treatment of fly ash with controlled T6 heat treatment to establish a reproducible link between processing, microstructure, and mechanical characteristics. Previous studies have mostly focused on either heat treatment optimization [13], [15], [16], or reinforcement effects [7], [8], [9], [10], [17], but they have not systematically examined the combined influence of electroless fly ash treatment and controlled T6 processing on tensile, impact, and fatigue performance.

The current research fills this gap by connecting the length of solution treatment and the temperature of artificial aging with the precipitation process ($\beta'' \rightarrow \beta' \rightarrow \beta$), the interfacial bonding strength, and the fracture mechanisms in Al6061–fly ash composites produced using stir casting. In environmentally friendly aluminium matrix composites, this integrated strategy establishes a replicable framework for optimizing the interaction between strength, toughness, and fatigue.

2. Material and methods

2.1 Material

Commercial Al6061 alloy ingots (ASTM B221 grade) were selected as the matrix material because of their well-known precipitation hardening behaviour within the Al–Mg–Si system. The composite was designed with 89 wt.% Al6061, 10 wt.% fly ash particles, and 1 wt.% magnesium. Magnesium was intentionally included as a wetting agent to improve interfacial bonding and enhance load transfer efficiency between the aluminium matrix and the ceramic reinforcement. Fly ash obtained from a coal-fired power plant was processed through a 200-mesh sieve (~75 μm) to ensure a uniform particle size distribution.

2.2 Composite preparation

The composite material was synthesized using a controlled stir casting method [1], [4]. The Al6061 alloy was heated to 700 ± 10°C in a resistance furnace until fully molten. Once the alloy was fully liquefied, magnesium was added and mechanically stirred for 5 minutes, followed by a gradual incorporation of coated fly ash particles while continuously stirring to ensure even distribution. The molten composite was then poured into a preheated steel mold at 300°C to reduce thermal gradients and prevent porosity. Solidification took place under ambient conditions.

To enhance mechanical properties through precipitation strengthening, T6 heat treatment was performed. The procedure involved solution treatment at 510 °C for 1 hour and 2 hours, rapid quenching in oil at ambient temperature (~25 °C) to prevent early precipitation, and artificial aging at 120 °C, 140 °C, and 160 °C for 2 hours. The chosen aging temperatures aimed to address under-aged, peak-aged, and over-aged states, reflecting the precipitation sequence β" → β' → β in Al–Mg–Si based alloys [16], [18][19]. Oil at room temperature (about 25°C) was used for fast quenching, with an estimated cooling rate of 40–60°C/s, which was sufficient to maintain a supersaturated solid solution and prevent premature β-phase precipitation before artificial aging [18], [19], [20].

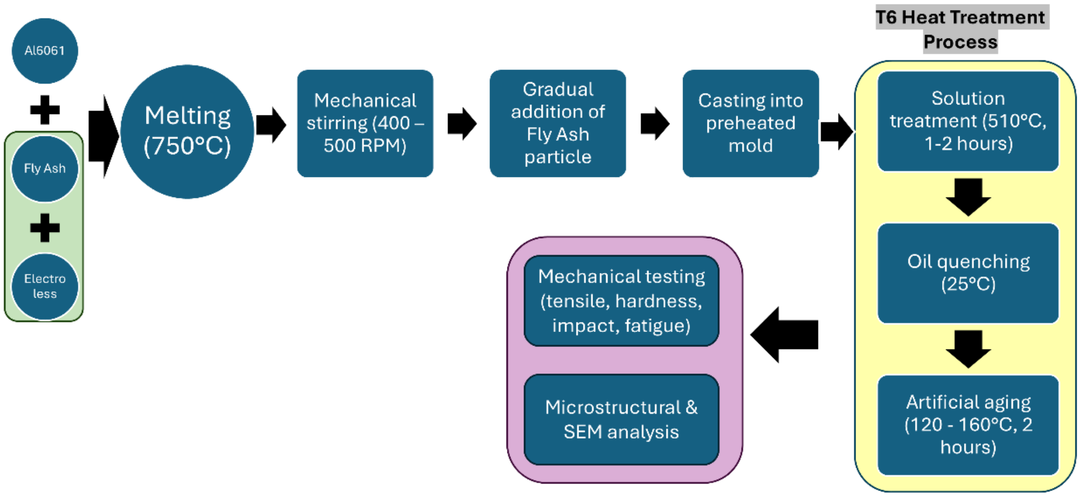

Figure 1. Representation of the experimental process

The heat treatment conditions were coded as follows: T6-A1: 510°C (1 hour) + aging 120°C (2 hours); T6-A2: 510°C (2 hours) + aging 120°C (2 hours); T6-B1: 510°C (1 hour) + aging 140°C (2 hours); T6-B2: 510°C (2 hours) + aging 140°C (2 hours); T6-C1: 510°C (1 hour) + aging 160°C (2 hours) and T6-C2: 510°C (2 hours) + aging 160°C (2 hours). Figure 1 presents a graphical workflow that outlines the complete process, including material preparation, composite manufacturing, T6 heat treatment, mechanical testing, and microstructural analysis.

2.3 Mechanical testing and microstructural characterization

Tensile testing of fly ash-reinforced Al6061 composites was conducted using a TARNO GROCKY, a universal testing machine with a maximum capacity of 1000 kN. Tensile test specimens were tested in accordance with the ASTM E8/E8M standards, with five samples tested for each T6 heat-treatment variation. Fatigue testing was conducted to determine the fatigue failure of the test specimen in accordance with ASTM E466. The impact test specimens used are in accordance with the ASTM E23 standard. Rockwell hardness testing uses a diamond cone to indent specimens under preload. After equilibrium is reached, the indenter depth through the specimen is recorded and used as the reference position. With the minor load still active, an additional (large) load is imposed on the indenter test specimen. Impact testing used the Charpy method with specimens in accordance with the ASTM E23 standard, which had a square cross-sectional area (10 x 10 mm) and a V-45° notch with a base radius of 0.25 mm and a depth of 2 mm. For each material condition, three cast samples were produced. The recorded numbers represent the average of findings from mechanical testing, conducted on five samples under each condition.

Material characterization involves several techniques to assess the properties and structure of composites. Microstructural analysis and Scanning Electron Microscopy (SEM) were conducted by using SEM instrument from FEI Brand, Inspect-S50, 2012, Hillsboro, Oregon, US. The obtained data were used to visually and qualitatively analyze the surface topology of composite materials. By using specific magnifications, these methods allow observation of the shape of the composite reinforcement and identification of voids or pores present in the material, upon fatigue fracture.

3. Results and discussion

3.1 Microstructural analysis

The microstructure of the fly ash-reinforced Al6061 composite after T6 heat treatment is shown in Figure 2. The material's tensile strength, fatigue behavior, and fracture properties are significantly influenced by the detected microstructural changes. In Figures 2(a)-(b) (T6-A1 and T6-A2), the fly ash particles are evenly distributed within the aluminium matrix, along with small precipitates generated during the T6 aging process. According to tensile test results [1], [13], the increase in tensile strength may be attributed to the presence of small Mg_2Si precipitates, which hinder dislocation motion and improve load transfer between the matrix and the reinforcement, thus strengthening the matrix.

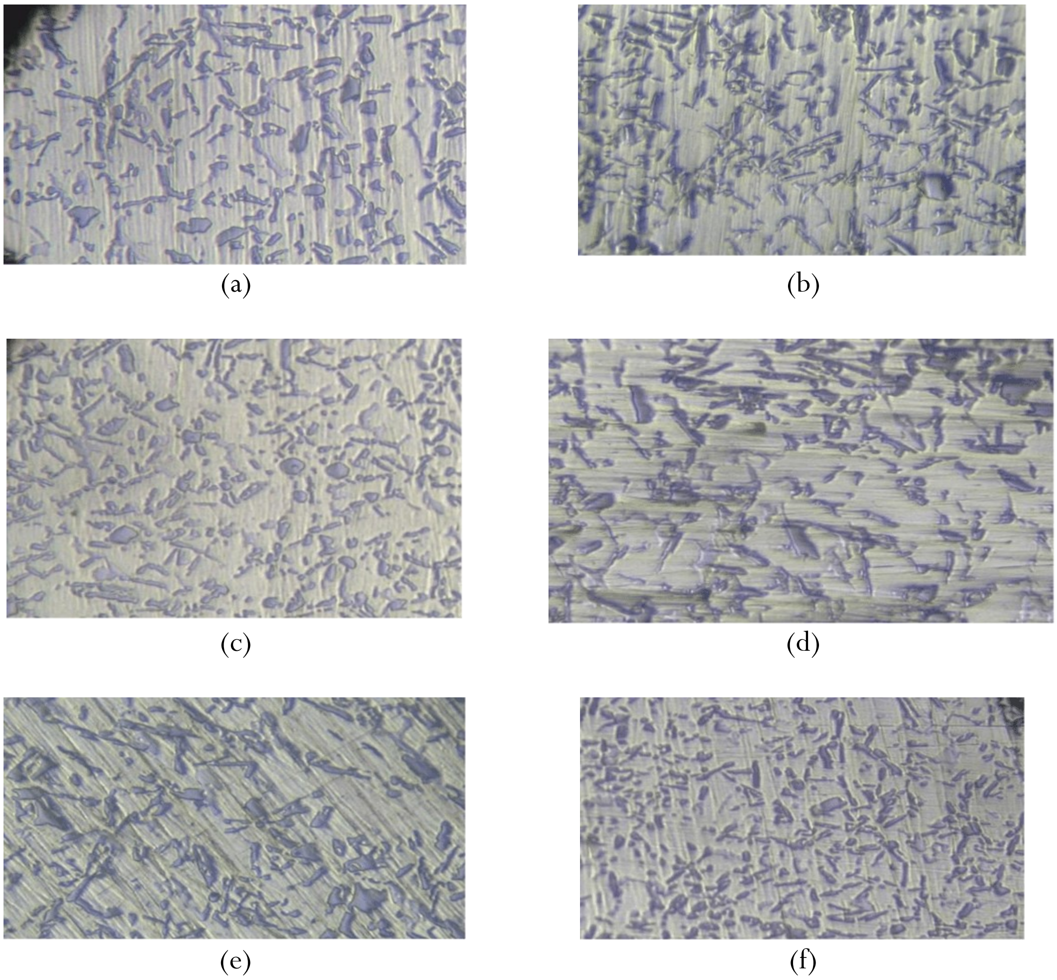

Figure 2. Microstructure of fly ash-reinforced Al6061 heat-treated samples (a) T6-A1, (b) T6-A2, (c) T6-B1, (d) T6-B2, (e) T6-AC1, and (f) T6-C2

The precipitates are slightly coarser, and there is some particle alignment, as shown in Figures 2(c) and 2(d) (T6-B1 and T6-B2). These characteristics can result in local stress concentrations that promote crack initiation under cyclic loading, which is consistent with the low fatigue life observed in the S-N curves, even if strengthening still occurs. Meanwhile, Figures 2(e)–(f) (T6-C1 and T6-

C2) illustrate more variable particle dispersion and local aggregation, which can accelerate crack formation and reduce load transfer efficiency.

These microstructural conditions support SEM fracture observations, where samples with a more uniform microstructure exhibit ductile fracture characterized by dimples, while samples with particle clusters exhibit particle pullout and mixed fracture features. This suggests that fatigue cracks first form at particle clusters or the particle-matrix interface before propagating throughout the aluminium matrix [5], [10]. These conditions cause local stress concentrations and accelerate crack initiation and propagation, thereby reducing tensile strength, impact energy, and fatigue life, as has also been reported for aluminium–fly ash composites and other Al–Mg–Si-based AMCs [3], [21]. On the other hand, a ductile fracture mechanism is observed under ideal T6 conditions, characterized by dimples of varying sizes, indicating considerable plastic deformation prior to failure. The explanation for this phenomenon is the fine and uniform precipitation of Mg_2Si during solution treatment and aging, as well as the enhanced interfacial bonding quality of the fly ash particles with the Al6061 matrix. According to prior studies, the best Mg_2Si precipitation enhances dislocation mobility inhibition, load transfer efficiency, and resistance to crack propagation, which in turn improves the tensile strength, hardness, impact toughness, and fatigue performance of Al–Mg–Si alloys and their composites [9], [22].

3.2 Tensile strength

Figure 3 illustrates that the tensile test findings, which show that the T6 heat treatment has a considerable strengthening effect over the untreated alloy (N-T6). The N-T6 condition exhibits ductile deformation behavior with strain hardening, with a yield strength of approximately 100 MPa, a tensile strength of approximately 268 MPa, and an elongation of approximately 10%. The T6 treatment results in a significant trade-off between strength and ductility, as seen by the increase in yield strength to 135–155 MPa, tensile strength to 270–305 MPa, and elongation decrease to 3–4.5%.

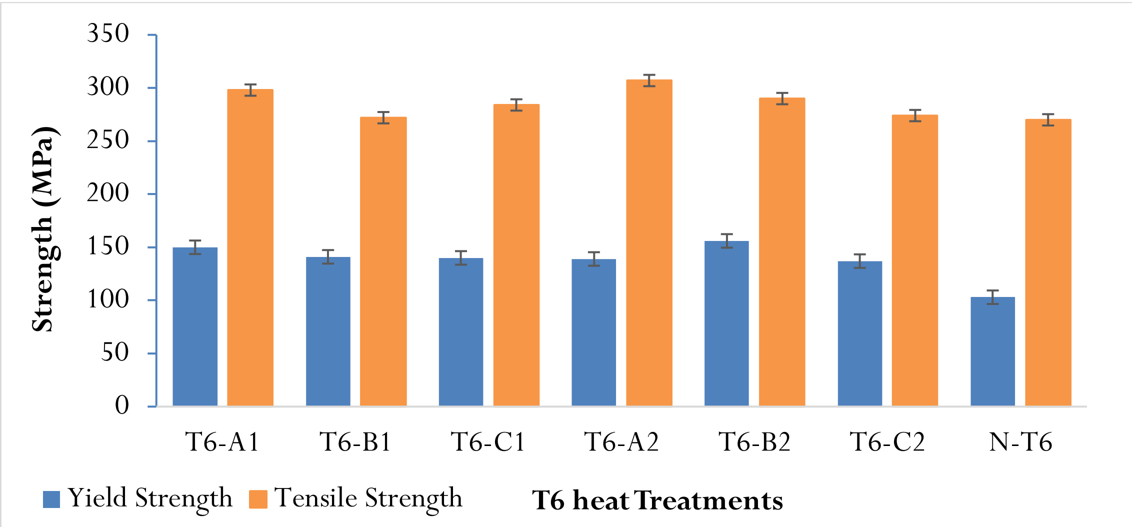

Figure 3. The yield and tensile strength of Al6061 composite with fly ash reinforcement heat-treated T6

T6-A2 (UTS 305 MPa; YS 155 MPa) produced the best results, with a 13–14% increase in tensile strength and a more than 50% increase in yield strength as compared to N-T6. This hardening aligns with the precipitation hardening mechanism described for aluminium-based systems [1], [2], [3], [4], [5], in which little, evenly dispersed precipitates effectively prevent dislocation motion. The excellent response of T6-A2 suggests that its aging characteristics are approaching ideal conditions,

as indicated by perfect precipitate size and coherence. Due to precipitation hardening caused by excessive aging, which lowers the efficiency of dislocation-particle interactions [7], [8], [9], [10], [11], [12], [13], T6-C2 (UTS 270 MPa; YS 135 MPa), on the other hand, has a lower strength.
The stress-strain curves further corroborate this perspective. The N-T6-treated sample exhibited significant deformation up to approximately 10% strain, indicating that the strengthening is primarily due to precipitation-driven dislocation anchoring rather than strain hardening, whereas the T6-treated specimen fractured at approximately 4% strain with little plastic flow. The maximum tensile strength (UTS) of 305 MPa, which was attained, is at the higher end of the reported range for similar T6 treatment systems [16], [23], [24], [25], demonstrating the effectiveness of microstructural optimization during the applied aging duration. In the T6 route, the yield strength may be increased by more than 50% through appropriate changes in aging parameters, as shown in this quantitative study, while the tensile strength remains above 300 MPa. This results in an almost ideal reinforcement environment in a short processing time that has not been investigated before.

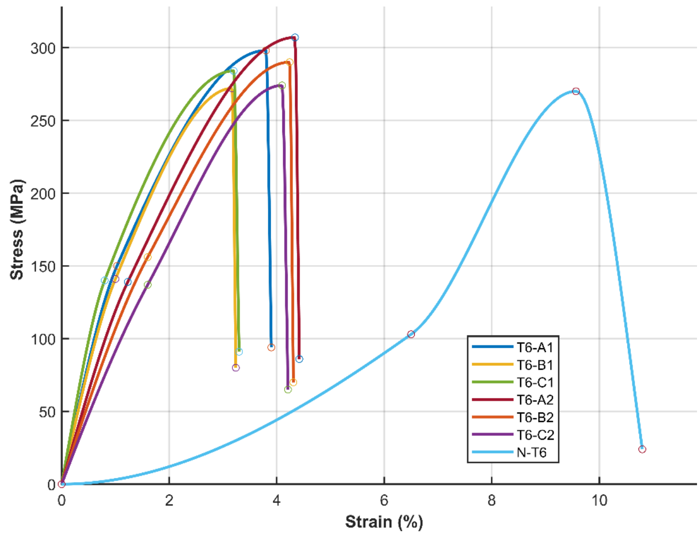

Figure 4. Engineering stress-strain curve (Interpolated) of Al6061 composite with fly ash reinforcement heat-treated T6

Figure 4 shows that the T6 treatment clearly exhibits a strengthening effect through a controlled decrease in ductility accompanied by a significant increase in yield strength and maximum tensile strength (UTS), compared to the N-T6 condition. With little resistance to dislocation motion, the untreated samples exhibit predominantly plastic deformation and a low yield strength value (103 MPa) but an exceptionally high strain capacity ($\varepsilon_f \approx 10.8\%$). On the other hand, all T6-treated samples exhibit significantly larger yield strength (137–156 MPa) and UTS (272–307 MPa), indicating effective precipitation strengthening. The A2 condition produces a maximum UTS (307 MPa) with a relatively high uniform strain and fracture ($\varepsilon_u \approx 4.34\%$, $\varepsilon_f \approx 4.42\%$), indicating an ideal balance between strain hardening and ductility. In contrast, B2 exhibits the highest yield strength (156 MPa) but reduced fracture strength (70 MPa), resulting in higher initial resistance to dislocation but earlier strain localization after constriction.

The significant decrease in ductility between the N-T6 and T6 conditions indicates the production of small, cohesive β'' precipitates that efficiently impede dislocation movement, leading to a higher work hardening rate but lower plastic strain capacity. Further variations between the A, B, and C series indicate a progression along the precipitation sequence β'' → β' → β, where the peak aging state (A2/B2) maximizes strength, while small decreases in strength or fractured stress (e.g., C2) indicate premature aging and precipitation hardening. It is well established that precipitation strengthening in aluminium matrix composites and Al-Mg-Si alloys suggests that the mechanical behavior is governed by precipitation-controlled dislocation anchoring and strain hardening behavior [13], [19], [26].

3.3 Hardness Rockwell

Figure 5 shows the hardness test results for aluminium alloy composites reinforced with fly ash and magnesium, both without treatment (N-T6) and following T6 heat treatment. The shown value represents the average across all variations in heat treatment duration. The hardness measurement for the untreated composite is 70.3 HRB. This value is lower than the hardness of the composite that underwent heat treatment. This value is lower than the hardness of the heat-treated composite. The variation in hardness is associated with changes in the matrix microstructure and the interfacial bonding between the aluminium matrix and fly ash reinforcement after heat treatment. SEM fractography revealed that the non-heat-treated composite exhibited irregular fracture features and localized porosity. In contrast, the heat-treated composite showed a more uniform fracture surface with improved matrix–reinforcement bonding.

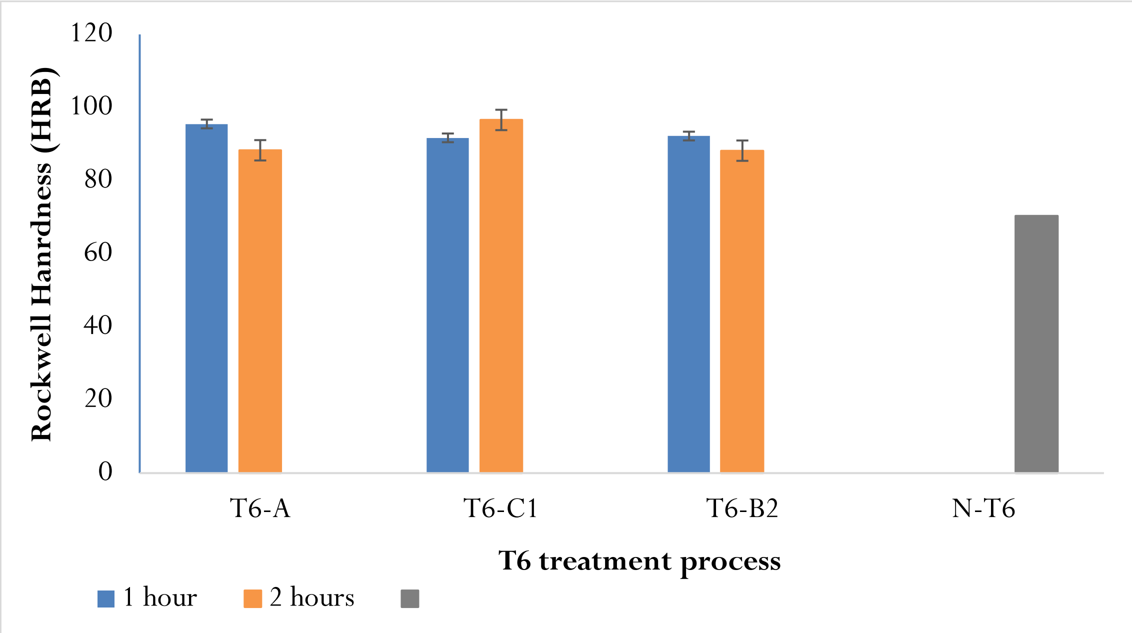

Figure 5. Rockwell Hardness versus heat treatment T6 and without heat treatment T6

For composites subjected to T6 heat treatment and artificial aging at 120°C, 140°C, and 160°C for durations of 1 and 2 hours, the hardness value increased by approximately 31.0% compared with the untreated composite, rising from 70.3 HRB to 92.10 HRB. The hardness characteristic relies on the bonding strength of aluminium and ceramic materials [2], [7], [10], along with the aspect ratio that enhances adhesion at the interface between the fibre and the matrix. Consequently, this treatment has the potential to significantly improve the mechanical characteristics of the composite.

Meanwhile, in composites with T6 heat treatment with artificial aging at temperatures of 120°C, 140°C and 160°C for 1 hour and 2 hours, it was found that the hardness decreased by 4% and 9%, namely from 95.5 HRB to 91.7 HRB, and from 96.6 HRB to 88.2 HRB. The highest hardness was observed in the composite that received T6 treatment at an artificial aging temperature of 120°C for 2 hours. Increasing the hardness of aluminium alloys with fly ash and magnesium reinforcements during heat treatment affects the microstructural morphology of the aluminium alloy, where the morphology of the fly ash crystals changes from smooth to rough.

Prior research on aluminium–fly ash and aluminium–ceramic composites [10], [14] confirms the observed improvement in hardness and tensile strength following T6 heat treatment. In the previous work [13], similar trends were observed, showing that precipitation hardening in T6-treated aluminium matrix composites dramatically increases yield and ultimate tensile strength by producing finely dispersed strengthening precipitates, while improved interfacial bonding between the matrix and ceramic reinforcement enhances more effective load transfer [4], [12], [19]. The hardening effect can be explained by a combination of precipitation hardening and particle-induced dislocation pinning, which together increase resistance to plastic deformation and delay crack initiation under tensile loading [19], [26]. However, the decrease in ductility seen in this research is also in line with earlier findings for particulate-reinforced metal matrix composites, where the presence of hard particles and a greater precipitate density limit matrix plasticity and encourage earlier micro void nucleation at the particle–matrix interface, resulting in a reduction in elongation to failure [2], [5], [10].

3.4 Impact energy

Figure 6 shows the impact energy values derived at 30 °C and 100 °C demonstrate a clear dependence on the precipitation state formed during T6 therapy and a significant correlation with the tensile behavior.

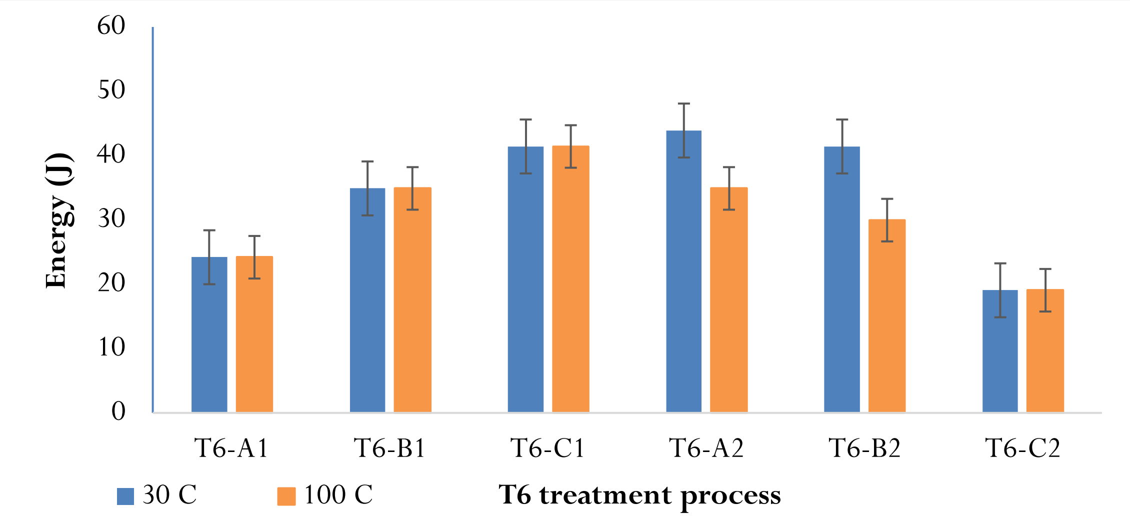

Figure 6. Impact energy of Al6061 composite with fly ash reinforcement heat-treated T6

The maximum impact energy is observed in A2 (~43 J) and C1/B2 (~41 J) at room temperature, whereas C2 has the lowest value (~18 J), indicating a significant drop in energy absorption capacity upon overaging. The specimens with superior tensile qualities (A2 and B2), which are distinguished by high yield strength and UTS, also retain high impact energy, indicating that peak-aged microstructures attain a favorable strength–toughness synergy rather than a straightforward trade-off. This behavior is consistent with the prevalence of tiny, coherent β'' precipitates, which successfully pin dislocations while maintaining enough ductility for the nucleation and development of stable micro voids. Conversely, the lower tensile strength and impact energy of C2 imply precipitate coarsening and transformation along the β'' → β' → β sequence, where loss of coherency and increased interparticle spacing reduce resistance to both plastic deformation and crack propagation. With only moderate strengthening, the comparatively stable response of C1 at 100 °C further suggests enhanced thermal stability connected with semi-coherent β' precipitates. In general, the combined tensile-impact response supports the idea that peak-aged, β''-dominated microstructures optimize both strength and energy absorption capability, while progression towards equilibrium β (Mg_2Si) and β' phases causes a gradual mechanical breakdown, which is consistent with previously established precipitation-hardening and fracture mechanisms in aluminium matrix composites and Al-Mg-Si alloys as well as earlier composite studies using the T6 method [13]. In the aluminium matrix, this microstructural development encourages crack deflection, particle pull-out, and localized plastic deformation, all of which increase toughness [5], [13]. Over-aging, in which precipitate coarsening reduces matrix strain-hardening capacity and interfacial strength [10], [12], is associated with the minor drop in impact energy at a longer aging duration (2 hours). According to these findings, the impact behaviour of Al6061–fly ash composites is determined by a balance between precipitation strengthening and ductility, with the greatest toughness attained at intermediate aging conditions before over-aging predominates [14], [19].

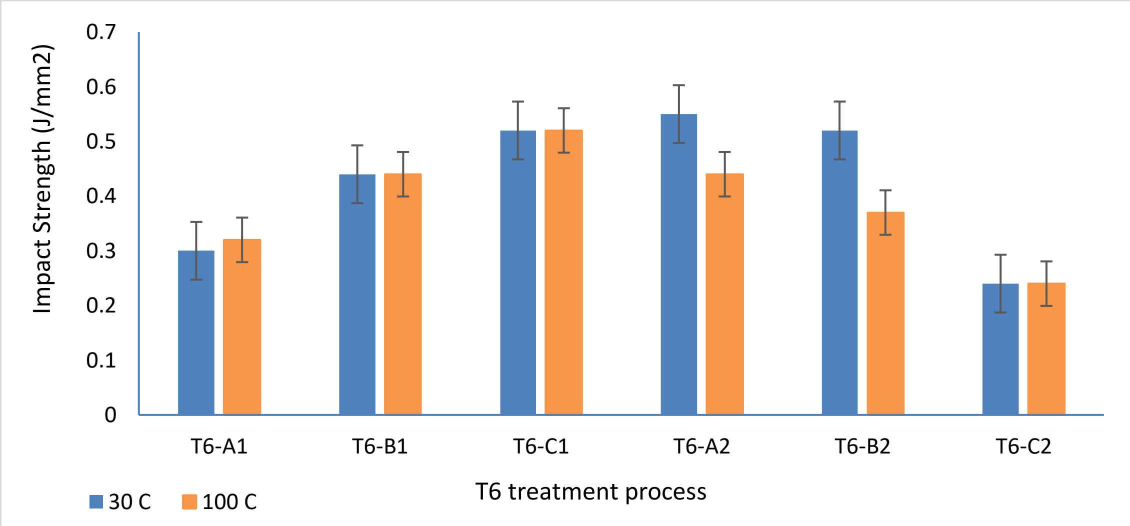

Figure 7. Impact strength of Al6061 composite with fly ash reinforcement heat-treated T6

Figure 7 shows the impact strength (J/mm²), indicating that the alloy's mechanical behaviour is significantly influenced by the precipitation state induced by the T6 treatment. The greatest impact strength is observed in A2 and C1 (0.52–0.55 J/mm²) at 30°C, followed by B2, while C2 shows the lowest value (0.23–0.25 J/mm²), suggesting a significant decline in crack resistance under overaged conditions. Importantly, the peak tensile condition (A2), which has the highest yield strength and UTS, also has the highest impact strength, demonstrating that the peak-aged microstructure has a synergistic improvement rather than a strength–toughness trade-off. This behaviour is compatible with a microstructure that is mostly made up of tiny, coherent β'' precipitates, which, while maintaining enough ductility for the nucleation of stable micro voids and resistance to crack growth, also maximizes dislocation pinning. This behaviour is associated with a more uniform particle distribution, improved interfacial bonding between fly ash and the aluminium matrix, and the formation of finely dispersed Mg_2Si precipitates that promote crack deflection and limited plastic deformation around reinforcement particles [2], [5], [10], [14].

3.5 Fatigue strength

Figure 8 presents the S–N curves of Al6061–fly ash MMCs subjected to T6 heat treatment with variations in solution time and artificial aging temperature. Specimens aged at 120–140 °C, particularly T6 510 °C–1 h + aging 140 °C–2 h, exhibit the highest fatigue life, retaining higher stress levels up to ~10^4–10^5 cycles. This behavior is consistent with the optimal balance between tensile strength and ductility, as previously shown by higher tensile strength (≈300 MPa) and moderate hardness values. SEM observations confirm a uniform distribution of fly ash particles, improved interfacial bonding due to Mg addition, and the presence of fine Mg_2Si precipitates, which effectively impede dislocation motion while still allowing limited plastic deformation. These microstructural features delay crack initiation and slow crack propagation under cyclic loading, explaining the superior fatigue resistance [2], [5], [10], [14].

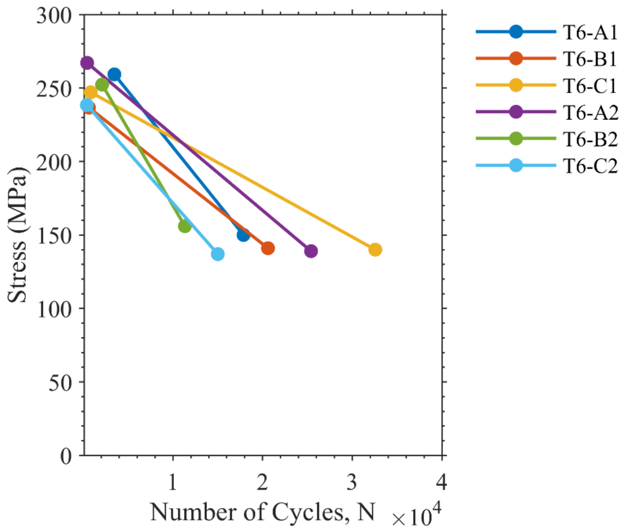

Figure 8. S-N curves of the heat-treated specimens with multiple variations of T6

In contrast, specimens aged at 160 °C, especially with longer solution or aging times, show a steeper decline in the S–N curve, indicating reduced fatigue life. Although these conditions still yield relatively high hardness, the over-aging effect leads to coarsening of Mg_2Si precipitates and increased particle–matrix debonding, as observed on SEM fracture surfaces. This microstructural degradation reduces impact energy and ductility, promoting early crack initiation at fly ash agglomerates and interfacial voids. The inverse relationship between hardness and fatigue life under over-aged conditions confirms that excessive precipitation strengthening compromises toughness and cyclic durability [7], [10], [12]. Overall, the fatigue behavior correlates strongly with tensile, hardness, and impact results, demonstrating that T6 heat treatment at moderate aging temperatures (120–140 °C) provides the most favorable combination of strength, toughness, and fatigue resistance for aluminium–fly ash MMCs [1], [5], [14].

3.6 Fracture surface observations

The tensile strength of the treated alloy (N-T6) increased significantly due to the T6 treatment, but its ductility decreased significantly. T6-A2 had the highest maximum tensile strength (UTS) of 307 MPa, which was 13.7% higher than N-T6 (270 MPa). The treated samples T6-A1 (298 MPa, +10.4%) and T6-B2 (290 MPa, +7.4%) also exhibited increases in strength. However, the T6 sample exhibited a decrease in elongation from 10.8% (N-T6) to 3.24–4.42%, representing an average ductility decrease of approximately 60%, indicating a strength-ductility trade-off due to precipitation. The SEM morphology of the fatigue fracture surface of a fly ash-reinforced Al6061 composite after T6 heat treatment is shown in Figure 9. The fracture morphology reveals the mechanisms of crack initiation and propagation during cyclic loading.

The fracture surfaces in Figure 9 (a) and (b) (T6-A1 and T6-A2) exhibit relatively small dimples and coalescence of micro-voids, indicating a primarily ductile fracture mechanism [1], [2], [5]. The uniform dimples indicate strong interfacial bonding between the fly ash particles and the aluminium matrix, which prolongs crack initiation and enhances fatigue resistance. This condition is consistent with the increased tensile strength and longer fatigue life observed in the S–N curves. Previous investigations have reported similar ductile fracture behavior in aluminium matrix composites [1], [11], [13].

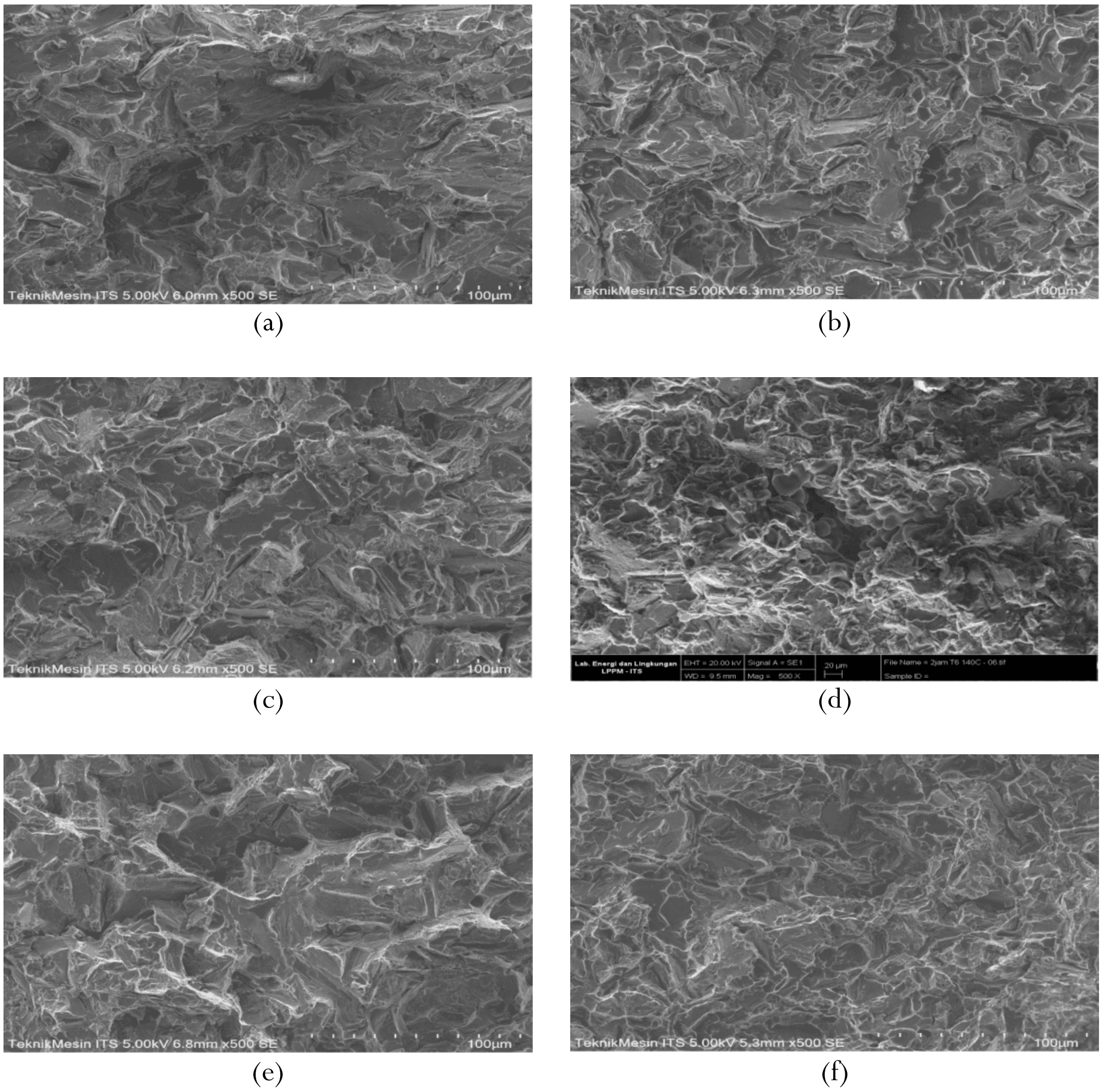

Figure 9. Morphology of fatigue fracture surfaces on Al6061-fly ash: (a) T6-A1, (b) T6-A2, (c) T6-B1, (d) T6-B2, (e) T6-C1, (f) T6-C2

The fracture surfaces in Figure 9(c) and (d) (T6-B1 and T6-B2) exhibit a combination of characteristics, including dimples and low cleavage-like areas. These characteristics indicate a shift from ductile to quasi-brittle fracture caused by local stress concentrations around the reinforcing particles, which accelerate crack nucleation under cyclic loading [5], [10]. Meanwhile, Figures 9(e) and (f) show more voids and signs of particle pullout, indicating the debonding of the interface between the aluminium matrix and fly ash particles. The lower fatigue strength observed in the S-N curves is explained by the fact that these defects act as crack initiation sites and promote faster crack propagation. In ceramic particle-reinforced aluminium matrix composites, a similar fatigue crack initiation process has been observed at the particle-matrix interface [7], [12], [27], [28], [29], [30].

4. Conclusion

The distribution and hardening of precipitation produced by the T6 heat treatment significantly impact the mechanical properties of Al6061–fly ash metal composites, as demonstrated in this study. Yield strength, ultimate tensile strength, hardness, impact energy, and fatigue resistance all significantly improved with the T6 heat treatment at 510°C followed by controlled artificial aging compared to the untreated condition. Ideal mechanical performance was achieved when the solution was treated for 1 hour at 510°C and then aged for 2 hours at 140°C, resulting in the best balance between strength and toughness. Microstructural and fractographic studies revealed that the peak condition favored the production of small, uniformly distributed Mg2Si precipitates and enhanced particle-matrix interfacial contact, leading to ductile fracture behavior characterized by well-developed grooves. Conversely, the over-aging condition caused rapid hardening and a partial loss of coherence, resulting in decreased impact energy and fatigue life due to earlier initiation of fracturing and local strain concentration. These findings emphasize that aluminium matrix composites with improved structural qualities can be prepared by combining sustainable fly ash reinforcement with an ideal T6 heat treatment. For the fabrication of affordable and environmentally friendly aluminium-based composites for structural and tribological applications, a favorable processing–microstructure–property relationship provides a framework within which to develop.

Author's declaration

Author contribution

Zainun Achmad: Conceptualization, Methodology, Investigation, Formal analysis, Data curation, Writing – original draft. **Al Emran bin Ismail**: Methodology, Validation, Supervision, Project administration, Writing – review & editing. **Harjo Seputro**: Formal analysis, Validation, Writing – review & editing. **Eka Marliana**: Data curation, Visualization, Writing – review & editing.

Funding statement

The publication of this research finding has been made possible through the financial support of Universitas 17 Agustus 1945 Surabaya.

Data availability

Data will be made available on request.

Acknowledgements

The authors would like to thank the Materials Laboratory of Universitas 17 Agustus 1945 Surabaya for technical support during specimen preparation and testing.

Competing interest

The authors declare no competing interests.

Ethical clearance

This research does not involve human or animal subjects, so an ethics document is not required.

AI statement

This article is the author's original work, written from original research, and no sections or figures were generated by AI. The language use of this article has been checked and verified by an English language expert.

Publisher's and Journal's note

Universitas Negeri Padang as the publisher, and Editor of Teknomekanik state that there is no conflict of interest towards this article publication.

References

[1] D. B. Miracle, "Metal matrix composites - From science to technological significance," *Compos. Sci. Technol.*, vol. 65, no. 15-16 SPEC. ISS., pp. 2526–2540, Dec. 2005, https://doi.org/10.1016/j.compscitech.2005.05.027

[2] K. Muqtadar Ali Khan, V. V.D. Sahithi, and K. Vijaya Krishna Varma, "Experimental investigation of mechanical and fracture behaviour of casted alumina (AA6061-SiC-flyash) metal matrix composites," in *Materials Today: Proceedings*, Elsevier Ltd, 2021, pp. 528–538. https://doi.org/10.1016/j.matpr.2020.10.742

[3] O. O. Barah, I. Bori, A. J. Otaru, and Z. A. A. A. Zaid, "Processing Optimization of Sustainable AA6061–Fly Ash Composites by Compocasting," *ACS Omega*, vol. 11, no. 4, pp. 6647–6656, Feb. 2026, https://doi.org/10.1021/acsomega.5c11742

[4] P. P. Ikubanni, M. Oki, A. A. Adeleke, and P. O. Omoniyi, "Synthesis, physico-mechanical and microstructural characterization of Al6063/SiC/PKSA hybrid reinforced composites," *Sci. Rep.*, vol. 11, no. 1, Dec. 2021, https://doi.org/10.1038/s41598-021-94420-0

[5] U. R. Kanth, P. S. Rao, and M. G. Krishna, "Mechanical behaviour of fly ash/SiC particles reinforced Al-Zn alloy-based metal matrix composites fabricated by stir casting method," *Journal of Materials Research and Technology*, vol. 8, no. 1, pp. 737–744, Jan. 2019, https://doi.org/10.1016/j.jmrt.2018.06.003

[6] Z. A. Karmo Main and A. E. Ismail, "Potential Applications of Fly-Ash and Sisal Hybrid Fibre Reinforced Plastic Composites," *International Journal of Engineering Trends and Technology*, vol. 68, no. 7, pp. 34–41, 2020, https://doi.org/10.14445/22315381/IJETT-V68I7P206S

[7] R. J. Shetty *et al.*, "Effect of metallic reinforcement and mechanically mixed layer on the tribological characteristics of Al-Zn-Mg alloy matrix composites under T6 treatment," *Cogent Eng.*, vol. 10, no. 1, 2023, https://doi.org/10.1080/23311916.2023.2200900

[8] N. Nanjayyanamat, R. Sugandhi, and S. Balanayak, "Mechanical Properties of Fly Ash Reinforced Aluminium 6061 Composite," *IOSR Journal of Mechanical and Civil Engineering*, pp. 55–59, 2011, [Online]. Available: https://www.iosrjournals.org/iosr-jmce/papers/Conf-17026-2017/Volume-3/11.%2055-59.pdf

[9] J. David Raja Selvam, D. S. Robinson Smart, and I. Dinaharan, "Microstructure and some mechanical properties of fly ash particulate reinforced AA6061 aluminum alloy composites prepared by compocasting," *Mater. Des.*, vol. 49, pp. 28–34, 2013, https://doi.org/10.1016/j.matdes.2013.01.053

[10] A. M. Razzaq, D. L. Majid, M. R. Ishak, and U. M. Basheer, "Effect of fly ash addition on the physical and mechanical properties of AA6063 alloy reinforcement," *Metals (Basel).*, vol. 7, no. 11, Nov. 2017, https://doi.org/10.3390/met7110477

[11] S. A. Sajjadi, H. R. Ezatpour, and H. Beygi, "Microstructure and mechanical properties of Al-Al2O3 micro and nano composites fabricated by stir casting," *Materials Science and Engineering: A*, vol. 528, no. 29–30, pp. 8765–8771, 2011, https://doi.org/10.1016/j.msea.2011.08.052

[12] M. Kok, "Production and mechanical properties of Al2O3 particle-reinforced 2024 aluminium alloy composites," *J. Mater. Process. Technol.*, vol. 161, no. 3, pp. 381–387, Apr. 2005, https://doi.org/10.1016/j.jmatprotec.2004.07.068

[13] A. Baradeswaran and A. Elaya Perumal, "Study on mechanical and wear properties of Al 7075/Al2O 3/graphite hybrid composites," *Compos. B Eng.*, vol. 56, pp. 464–471, 2014, https://doi.org/10.1016/j.compositesb.2013.08.013

[14] C. S. Tsao, C. Y. Chen, U. S. Jeng, and T. Y. Kuo, "Precipitation kinetics and transformation of metastable phases in Al-Mg-Si alloys," *Acta Mater.*, vol. 54, no. 17, pp. 4621–4631, Oct. 2006, https://doi.org/10.1016/j.actamat.2006.06.005

[15] K. Choi, S. Lee, and D. Bae, "Natural and Artificial Aging Effects on the Deformation Behaviors of Al–Mg–Zn Alloy Sheets," *Materials*, vol. 17, no. 18, Sep. 2024, https://doi.org/10.3390/ma17184478

[16] M. I. A. Habba *et al.*, "Microstructural evolution and strengthening mechanisms in Cu-coated cBN reinforced aluminum nanocomposites," *Journal of Materials Research and Technology*, vol. 38, pp. 3291–3309, Sep. 2025, https://doi.org/10.1016/j.jmrt.2025.08.113

[17] H. Seputro, S. R. Bintoro, D. Ariawan, E. Surojo, and Triyono, "Enhancing AA6061–Bottom Ash Composites: Role of Heat Treatment on Properties and Dimensional Stability," *Civil Engineering Journal (Iran)*, vol. 11, no. 11, pp. 4864–4885, Nov. 2025, https://doi.org/10.28991/CEJ-2025-011-11-023

[18] R. Lazarova, L. Anestiev, Y. Mourdjeva, K. Valuiska, and V. Petkov, "Microstructural Evolution, Strengthening Mechanisms, and Fracture Behavior of Aluminum Composites Reinforced with Graphene Nanoplatelets and In Situ–Formed Nano-Carbides," *Metals (Basel).*, vol. 15, no. 3, Mar. 2025, https://doi.org/10.3390/met15030285

[19] H. Jin, D. Tie, and R. Guan, "Precipitation behavior during re-aging of Al-Mg-Si-Cu alloy," *Mater. Des.*, vol. 220, Aug. 2022, https://doi.org/10.1016/j.matdes.2022.110883

[20] R. Almeida Rodrigues *et al.*, "Effect of Different T6 Heat Treatment Conditions on the Microstructure and Mechanical Properties of Al-7%Si-0.35% Mg (A356) Alloy for Use in Motorcycles," *Metals (Basel).*, vol. 15, no. 7, Jul. 2025, https://doi.org/10.3390/met15070692

[21] L. Shyam, K. Sudhir, K. Ajay, P. Lalman, and Aniruddha, "Fabrication and Characterization of Hybrid Metal Matrix Composite Al-2014/SiC/Fly Ash Using Stir Casting Process," *Mater. Today Proc.*, vol. 49, no. 8, pp. 3155–3163, 2022, https://doi.org/10.1016/j.matpr.2020.11.168

[22] M. Gazizov, C. D. Marioara, J. Friis, S. Wenner, R. Holmestad, and R. Kaibyshev, "Precipitation behavior in an Al–Cu–Mg–Si alloy during ageing," *Materials Science and Engineering: A*, vol. 767, Nov. 2019, https://doi.org/10.1016/j.msea.2019.138369

[23] B. H. Lee, S. W. Park, S. K. Hyun, I. S. Cho, and K. T. Kim, "Mechanical properties and very high cycle fatigue behavior of peak-aged AA7021 alloy," *Metals (Basel).*, vol. 8, no. 12, Dec. 2018, https://doi.org/10.3390/met8121023

[24] L. F. Demisie *et al.*, "Experimental analysis on the mechanical properties of Al6061 based hybrid composite reinforced with silicon carbide, bagasse fly ash and aloe vera ash," *Discover Applied Sciences*, vol. 6, no. 9, Sep. 2024, https://doi.org/10.1007/s42452-024-06192-7

[25] L. Stemper, M. A. Tunes, R. Tosone, P. J. Uggowitzer, and S. Pogatscher, "On the potential of aluminum crossover alloys," *Progress in Materials Science*, vol. 124. Elsevier Ltd, Feb. 01, 2022. https://doi.org/10.1016/j.pmatsci.2021.100873

[26] T. S. Liu, B. X. Dong, H. Y. Yang, F. Qiu, S. L. Shu, and Q. C. Jiang, "Review on role of intermetallic and ceramic particles in recrystallization driving force and microstructure of wrought Al alloys," *Journal of Materials Research and Technology*, vol. 27. Elsevier Editora Ltda, pp. 3374–3395, Nov. 01, 2023. https://doi.org/10.1016/j.jmrt.2023.10.098

[27] P. X. Zhang, H. Yan, W. Liu, X. L. Zou, and B. B. Tang, "Effect of T6 heat treatment on microstructure and hardness of nanosized Al2O3 reinforced 7075 aluminum matrix composites," *Metals (Basel).*, vol. 9, no. 1, Jan. 2019, https://doi.org/10.3390/met9010044

[28] G. Rodríguez-Cabriales *et al.*, "Synergistic Effects of Sub-Micron WC Reinforcement and T6 Heat Treatment on the Evolution of Microstructure and Mechanical Behavior in Al–Cu–Mg Composites Fabricated Through Powder Metallurgy," *Metals (Basel).*, vol. 15, no. 11, Nov. 2025, https://doi.org/10.3390/met15111216

[29] H. R. Channar, B. Ullah, M. S. Naseem, J. Akhter, A. Mehmood, and M. Aamir, "Mechanical Properties and Microstructural Investigation of AA2024-T6 Reinforced with Al2O3 and SiC Metal Matrix Composites," *Eng*, vol. 5, no. 4, pp. 3023–3032, Dec. 2024, https://doi.org/10.3390/eng5040157

[30] Z. Achmad, E. Santoso, and A. Jalil, "Analysis of The Effect of Cooling Media Variation And Variation of Cooling Media Temperature on T6 Process Solution Treatment on Shape And Propeler Dimension Changes From Coal Based ALUMINUM-ASH Composite Materials," in *SNTTM XVI*, 2018. Page. 161-165. https://prosiding.bkstm.org/prosiding/2018/RM-30.pdf